

UDC 521.312.4 : 521.4 : 521.6 : 551.510.53 :
551.557 : 629.19.077.3 : 629.192.7

ROYAL AIRCRAFT ESTABLISHMENT

Technical Report 71202

September 1971

ANALYSIS OF THE ORBIT OF COSMOS 268 ROCKET (1969-20B)

by

D. G. King-Hele

A. N. Winterbottom

SUMMARY

The orbit of Cosmos 268 rocket (1969-20B) has been determined at 28 epochs during its 342-day life, with the aid of the PROP5 orbit refinement program. All available observations were used, including 16 from the Hewitt camera at Malvern, 28 from the 200-mm camera at Meudon, 56 from the kinetheodolite at the Cape Observatory, 700 visual observations from volunteer observers, 500 US Navy observations and 200 British radar observations. The orbits are of very good accuracy for such a high-drag satellite, most of the values of inclination having standard deviations less than 0.002° . The most accurate orbits are those utilizing photographic observations, and the best of these has standard deviations of 0.00001 in eccentricity and 0.0001° in inclination.

The values of inclination obtained, after correction to allow for the effects of other perturbing forces, have been analysed to determine zonal wind speeds in the upper atmosphere at heights a little above perigee (230-250 km) averaged over latitudes up to about 25° . The results show a clear distinction between the wind at night (21 h to 03 h local time), which is west-to-east with an average speed of 140 ± 50 m/s, and the wind by day (04 h to 19 h), which is east-to-west with an average speed of 110 ± 50 m/s.

Departmental Reference: Space 381

CONTENTS

	<u>Page</u>
1 INTRODUCTION	3
2 THE OBSERVATIONS	3
3 THE ORBITS	4
3.1 General review	4
3.2 Techniques for orbit improvement	5
3.3 Perigee height	6
3.4 Decay rate	7
4 UPPER-ATMOSPHERE WIND SPEEDS, FROM THE CHANGES IN INCLINATION	7
5 RESIDUALS OF THE OBSERVATIONS	10
6 CONCLUSIONS	12
Table 1 Orbital parameters for Cosmos 268 rocket (1969-20B) with standard deviations	13
Table 2 Values of Λ obtained	9
Table 3 Analysis of residuals for selected stations	11
References	15
Illustrations	Figures 1-4
Detachable abstract cards	-

1 INTRODUCTION

Cosmos 268 was launched on 5 March 1969 into an orbit inclined at 48.4° to the equator, with an initial orbital period of 109.1 minutes. Its final-stage rocket, designated 1969-20B, entered a similar orbit, with an initial perigee height 220 km and apogee height nearly 2200 km. This rocket, 8 m long and 1.65 m in diameter, was a good object for optical observation from Britain, its stellar magnitude at 45° elevation being about +2 near perigee and +5 near apogee. The orbit contracted rapidly because perigee was so low, and 1969-20B decayed on 11 February 1970. During its 342-day life the orbital period decreased by more than 20 minutes, so the decrease in orbital inclination caused by atmospheric rotation was expected to be quite substantial, perhaps as much as 0.1° . Consequently the orbit seemed promising for use in determining the upper-atmosphere rotation rate, and 1969-20B was given a high priority for observing by the British optical and radar tracking stations, including the Hewitt camera at Malvern.

The orbit of 1969-20B has been determined from all available observations with the aid of the RAE orbit determination program PROP¹ in the PROP5 version, at 28 epochs between 5 April 1969 and 10 February 1970. This Report describes the orbit determinations, and analyses the resulting values of inclination to determine atmospheric rotation rates at heights near 240 km.

2 THE OBSERVATIONS

Six groups of observations were available. The most accurate were those from the 600-mm Hewitt camera at Malvern. Although these observations do not exploit the full accuracy of the camera, because the plates are reduced by a quicker method than is used for geodetic work, the Hewitt camera observations are nevertheless usually accurate to about 2 seconds of arc. For 1969-20B there were 16 of these observations, from 4 plates.

The second group, almost as accurate, were the photographic observations from the 200-mm camera at Meudon. There were 28 of these observations, on 7 transits, with an accuracy of about 5 seconds of arc.

The next most accurate group of observations was that from the kine-theodolite at the Cape Observatory, South Africa, with accuracy of about $1\frac{1}{2}$ minutes of arc. These observations, 56 in number, were of particular importance because of their geographical location: since northern-hemisphere observations are usually predominant, the addition of a few accurate southern-hemisphere observations can greatly improve the orbital accuracy.

Observations from the other three sources, which made up the great majority of the data, were all of rather similar accuracy, between $1\frac{1}{2}$ and 5 minutes of arc in direction and (for radar only) between 1 and 2 km in range. The most numerous of these (over 700) were visual observations from the volunteer observers who report to the Radio and Space Research Station, Slough or the Moonwatch Division of the Smithsonian Astrophysical Observatory, and from the theodolites at Meudon and associated stations in France. Since most of the visual observations were made from latitudes between 48° and 52° , they had a strong influence in fixing the value of the orbital inclination, on those occasions when camera observations were not available.

Another major source of observations was US Navy data, kindly supplied by the US Naval Research Laboratory. More than 500 US Navy observations were used, and many of the orbit determinations would have been impossible without them.

The sixth category of observations comprised those from British radar stations, particularly the radar tracker at RRE, Malvern. These observations totalled nearly 200 and were particularly useful at the end of the satellite's life.

3 THE ORBITS

3.1 General review

The 28 orbits obtained are given in Table 1 on page 13. As usual with PROP, the epoch is at 0 h on the chosen day and the definitions of the main orbital elements are given below the table. In PROP the mean anomaly M is fitted by a polynomial of the form

$$M = M_0 + M_1 t + M_2 t^2 + M_3 t^3 + M_4 t^4 + M_5 t^5 \quad (1)$$

where t is the time, measured from the chosen epoch, and the number of coefficients M_2, M_3, \dots used is open to choice. With a high-drag orbit like that of 1969-20B, the best number of coefficients to use has to be found by trial and error. For 4 of the runs the best results were obtained by using M_0 to M_2 only; 13 of the runs required M_0 to M_3 ; 10 required M_0 to M_4 ; and for the last run, near the end of the life, the full complement of M_0 to M_5 was found to be necessary. The orbits given in Table 1 fit the observations well, with ϵ , the parameter measuring the goodness of fit, usually rather less than 1.

The 7 orbits which utilised Hewitt or Meudon camera observations are marked with asterisks in Table 1, and these can appropriately be discussed first. For one of these orbits, No.5, the supporting observations were unfortunately quite inadequate both in number and in geographical coverage, and the orbit obtained was rather mediocre. The remaining 6 orbits gave values of inclination which were of excellent accuracy, with the standard deviations ranging from 0.0001° and 0.0007° , corresponding to distances between 10 and 90 metres. One orbit, No.14, has the lowest standard deviations yet obtained for such a high-drag orbit ($M_2 = 1.3 \text{ deg/day}^2$), with sd in eccentricity of 0.00001 , corresponding to sd in perigee height of 70 m, and sd in inclination of 0.0001° . Orbit No.7, which utilizes 4 plates from the Meudon camera all within a time interval of 48 hours, has even lower sd for some of the parameters, 0.00006° for i , 0.001° for Ω and 0.0002 deg/day for M_1 ; but the observations are few in number (25) and are all from latitudes between 48° and 54° , so that there is more danger of bias which may considerably exceed the sd. Also, as would be expected with such limited orbital coverage, the sd in eccentricity is relatively large (0.00006).

The 21 orbits obtained without the aid of camera observations were of somewhat varied accuracy, depending on the number and geographical location of the observations. On 14 of these orbits (including the final one) the sd in inclination was between 0.0013° and 0.0020° , while the other 7 had values between 0.0022° and 0.0038° . Standard deviations in eccentricity range between 0.00001 and 0.00006 on all the orbits except run 9, for which the geographical coverage was very poor. The sd in the right ascension of the node was between 0.002° and 0.007° , again with the exception of run 9.

3.2 Techniques for orbit improvement

It was usually necessary to run the PROP program several times at each epoch, with each run involving a number of iterations in the refinement process, before arriving at the final orbits listed in Table 1. Quite often the first attempt would end in divergence, because the initial orbit, usually predicted from the previous epoch, was not accurate enough. On average, the first successful attempt needed about 10 iterations, the final convergence often being delayed because of the presence of observations which were in error by a fairly small amount and tended to be rejected one by one in successive iterations. Usually the first attempts were made with the parameters M_0 to M_3 in the polynomial for M , but it was often necessary to re-run with

M_0 to M_2 only, or with M_0 to M_4 , to see whether the fit was better with these sets of coefficients. The other main reason for re-runs was the survival of observations which 'looked wrong', but were not bad enough to be rejected by the computer. Observations are rejected if they have a residual greater than 3ϵ times the assumed error: but if, say, 5 out of 30 observations have weighted residual 3, their initial acceptance inevitably keeps ϵ greater than $\sqrt{45/30}$, i.e. greater than 1.2, thereby ensuring their survival.

When the 'final' orbits had been arrived at, and the values of inclination were plotted against time, it appeared that some values near the end of the life were out of step with the general trend. These orbits were re-examined and re-run with various modifications: the orbit eventually fitted the observations better - and better values of inclination were obtained - usually after omitting observations, either at the beginning or end of the set used, or at a time when irregularities in drag seemed to be spoiling the fit. All these difficulties are most probably due to the polynomial for M failing to fit the real drag, which was not only irregular but also very large, with M_2 greater than 2 deg/day.

3.3 Perigee height

Fig.1 gives an impression of the variations in perigee height. The crosses indicate values of $a(1 - e) - R$, i.e. the perigee 'height' with respect to the Earth's equatorial radius R ($= 6378.2$ km). The broken curve drawn through the crosses shows the oscillation in perigee distance produced by the odd zonal harmonics of the Earth's gravitational field. For a satellite with inclination 48.4° the amplitude of this oscillation² is 5.2 km. So, if we define a perigee height parameter, Q , by the equation

$$Q = a(1 - e) - R + 5.2 \sin \omega \quad \text{km} \quad (2),$$

Q should be constant apart from luni-solar perturbations and the gradual decrease in perigee height due to the effect of air drag. In Fig.1 the values of Q for the 28 orbits are indicated by circles, with sd when these are large enough to be visible: the values of Q are satisfactorily close to a smooth curve, though the rather steep initial slope of the curve is a little unexpected.

For a satellite with inclination 48° , like 1969-20B, the average Earth radius over a complete revolution is about 6372 km, so the average perigee height is about $Q + 6$ km.

3.4 Decay rate

The decay rate of 1969-20B due to air drag was rapid and variable, and Fig.2 gives values of

$$\frac{1}{2}\ddot{M} = M_2 + 3M_3t + 6M_4t^2 \quad (3),$$

where t is the time from epoch, over the time intervals covered by the observations used at each epoch. Fig.2 indicates the variability in drag from week to week, but does not show the day-to-day irregularities, which tend to be smoothed out by fitting a polynomial for M .

The two most severe magnetic storms during the lifetime of the satellite occurred on 15 May and 30 September 1969, and are marked in Fig.2 by double-headed arrows. Sharp increases in air density occur at the times of such magnetic storms and corresponding increases would be expected in \ddot{M} , which is directly proportional to the air density at heights near perigee. Fig.2 confirms that there are steep increases in \ddot{M} at these times: the two orbits affected (Nos.6 and 14) have the highest (positive) values of M_3 for any orbit up to No.23.

4 UPPER-ATMOSPHERE WIND SPEEDS, FROM THE CHANGES IN INCLINATION

Because the upper atmosphere is rotating, at approximately the same rate as the Earth, the aerodynamic force acting on a satellite has a component perpendicular to the orbit, which has the effect of reducing the inclination of the orbit to the equator as time goes on. For a high-drag satellite, atmospheric rotation is the most important force perturbing i , and if corrections are made to allow for luni-solar, odd zonal harmonic and tesseral harmonic perturbations, the changes in i give the atmospheric rotation rate and hence the wind speed in the region near the satellite's perigee.

Fig.3 shows the values of i from the 28 orbits in Table 1, with $\pm d$. These values were corrected, using the PROD computer program³, for the effects of zonal harmonic and luni-solar perturbations, which were calculated at 1-day intervals; and also corrected for the $J_{2,2}$ tesseral harmonic perturbations, which were always less than 0.0015° . The corrected values of inclination, with $\pm d$, are plotted in Fig.4. The theoretical curves for the change in inclination due to an atmosphere rotating at various constant rates (0.7, 0.8 1.4 rev/day) were then calculated by numerical integration of

the equation⁴ for $\frac{di}{dT}$ at intervals of 45° in ω (approximately 10 days in time) initially, and at closer intervals later in the satellite's life.

It immediately became apparent that the values of i in Fig.4 could not be fitted satisfactorily if the rotation rate Λ were kept constant: Λ had to be greater in the middle of the life than at the beginning or end. So the theoretical curve was divided into 3 sections, with breaks at what appeared to be the most suitable dates, namely MJD 40431 and 40500. At the first of these dates perigee was at southern apex ($\omega = 270^\circ$), and $\frac{di}{dT} = 0$, so the curve continues without any change in slope. The second break occurs when perigee was on the equator, and the inclination was decreasing most rapidly. The values of Λ (rev/day) which gave the best fit for the combined 3-part curve were judged to be: (1) $\Lambda = 0.8$; (2) $\Lambda = 1.3$; and (3) $\Lambda = 0.7$. The estimated errors in Λ are 0.1 (sd) for sections (1) and (2), and 0.15 for section (3), the error in section (2) being proportionately smallest - 8%, as against 12% for section (1) - because both its ends are 'fixed' by having to link up with the other sections.

Since it is quite likely that Λ varies with local time, a scale of local time is given at the top of Fig.4. It is not possible to specify an exact local time for which Λ applies, because (a) the effects of atmospheric rotation are appreciable over an arc of about 30° on each side of perigee (i.e. $\pm 1\frac{1}{2}$ hours approximately), and (b) the effects are greatest when perigee is near the equator and the curve in Fig.4 is at one of its points of maximum slope. Thus, to clarify the picture by somewhat oversimplifying it, the air is being sampled at local times about ± 2 hours from the local time at perigee at the equator crossing; and, by rather good luck, the successive equator crossings are at intervals of approximately 4 hours in local time, so that the whole spectrum of local time is covered, though with some bias towards the times when perigee crosses the equator. The scale at the top of Fig.4 indicates that in section (1) Λ applies for local times between 04 and 14 h; in section (2) between 21 h through midnight to 03 h; and in section (3) between 09 and 19 h*. These results apply at a height h of a scale height above the mean perigee height of the satellite: from Fig.1 the mean perigee height ($Q + 6$ km) decreases from about 225 km in section (1) to about 210 km in

*The point at MJD 40503 can conveniently be regarded as the end of section (2), with the point at MJD 40522 as the first in section (3).

section (3) and the scale height decreases correspondingly from about 32 km to about 29 km. These results are summarized in Table 2 below.

Table 2
Values of Λ obtained

	Dates	Local time at perigee	Λ rev/day	Height km
(1)	1969 Apr 5 - July 29	04-14 h	0.8 ± 0.1	250
(2)	1969 July 29 - Oct 6	21-03 h	1.3 ± 0.1	245
(3)	1969 Oct 6 - 1970 Feb 10	09-19 h	0.7 ± 0.15	230

These results, which may be regarded as averages over latitudes up to $\frac{1}{2}i$, that is up to 24° , strongly support the idea that the prevailing winds depend on local time. If the values in sections (1) and (3) are combined to give $\Lambda = 0.75 \pm 0.1$, there is a clear distinction between strong west-to-east winds averaging about 140 ± 50 m/s at night (21 h to 03 h) and east-to-west winds averaging about 110 ± 50 m/s by day (04 to 19 h). This result is in accord with the somewhat limited evidence from vapour-trail measurements⁵⁻⁸ and with previous orbital analyses^{9,10}. Most theoretical studies also suggest that in near-equatorial regions the strongest west-to-east winds are likely to occur in the late evening, between 20 h and 02 h (see, for example, Ref.11).

Hiller's orbit¹⁰ of Cosmos 307 rocket shows that the changes in wind direction occurred soon after the two most severe magnetic storms¹². This may be coincidence, and it may also be by chance that the two strongest geomagnetic disturbances during the lifetime of 1969-20B occurred at the beginning of sections where Λ was low. Obviously, the evidence is as yet far too tenuous to draw conclusions, but the link between geomagnetic disturbances and zonal wind speeds in the auroral zone, demonstrated by Rees¹³, may lead to some indirect influence at lower latitudes.

Since the local time at perigee in Fig.4 ranges over more than 24 h, it is possible to give a mean value of Λ averaged over 24 h of local time. The obvious choice of end points for this calculation is MJD 40334 and 40565: the equator crossings covered are then those occurring at about 17 h, 21 h, 01 h, 05 h and 10 h local time. Between MJD 40334 and 40565 the inclination decreases by the same amount as in Fig.4 (0.034°) if Λ is kept constant at a value of 0.9, with sd estimated as 0.1. This is the lowest mean value of

As so far obtained from orbital analysis at heights between 200 and 400 km, and is significantly lower than the value given by the mean curve in Ref.12.

It will be seen that the last four points in Fig.4 are appreciably above the curve. This may be due to the difficulty in determining accurate orbits with such high drag ($M_2 > 4 \text{ deg/day}^2$), but it is also worth noting that the orbit passed through 15th-order resonance with the Earth's gravitational field near MJD 40600. Such a passage through resonance produces a change in inclination which for the Ariel 3 satellite¹⁴ was 0.018° ; the corresponding change for 1969-20B cannot be calculated because it depends primarily on the coefficients $C_{19,15}$ and $S_{19,15}$ in the Earth's gravitational potential. However, the change seems unlikely to exceed 0.003° because 1969-20B passed through resonance so rapidly. Nevertheless an increase in i of 0.003° around MJD 40600 would help to explain why the last four points in Fig.4 were above the curve.

5 RESIDUALS OF THE OBSERVATIONS

The residuals of the observations, in the form of the observer's value minus that given by the fitted orbit at the time specified by the observer, have been printed out using the ORES computer program¹⁵ and have been sent to the individual observers. Table 3 gives the number of observations from stations with 5 or more accepted observations, with the rms residuals in minutes of arc, or km for the range measurements.

Table 3 calls for several comments. First, it should be noted that the directional residuals for the US Navy station 29 are geocentric and should be multiplied by a factor of about 5 to make them comparable with the other figures for directional accuracy. Second, it is possible that the most accurate observations, namely those from the Malvern and Meudon cameras, are more accurate than is suggested by the residuals, because this was a high-drag orbit for which a fit accurate to better than 2 seconds of arc, though often possible, cannot be guaranteed if the drag is irregular. Third, the proportion of rejections is rather high, and some of these are not necessarily bad observations: variations in drag on some days may have been so large that the polynomial for M was inadequate and good observations may have been rejected, particularly if they were isolated geographically. Fourth, the rms residuals do not give a realistic idea of the visual observer's capabilities because a few observations made in poor conditions (semi-daylight, cloud, haze, etc.) can outweigh a whole group of good observations. For example,

Table 3

Analysis of residuals for selected stations

Station	No. of observations		rms residuals			
	Total	Rejected	Range km	Minutes of arc		
				RA	Dec.	Total
1 US Navy	58	3	1.0	4.4	4.3	6.1
2 US Navy	50	3		3.9	3.4	5.1
3 US Navy	42	4		5.3	3.6	6.4
4 US Navy	38	1		4.2	3.5	5.5
5 US Navy	53	2		4.4	3.2	5.4
6 US Navy	51	4		5.7	4.5	7.2
29 US Navy	233	11		1.0*	0.7*	
414 Capetown	11	2		4.3	4.1	5.9
2265 Farnham	37	6		5.9	4.2	7.2
2295 Leyton	9	3		1.7	0.8	1.9
2303 Malvern Hewitt Camera	16	1	0.8	0.04	0.03	0.05
2304 Malvern Radar	115	1		2.5	3.0	
2344 Thames Ditton	5	0		1.6	1.6	2.3
2366 Earlyburn	13	1		3.5	3.1	4.7
2385 Stevenage 1	6	1		1.5	1.2	2.0
2403 Stevenage 3	23	3		2.1	1.4	2.5
2409 Ribbleton	69	4		3.8	2.0	4.3
2413 Norwich	29	7		7.2	4.9	8.7
2414 Bournemouth	80	11		5.3	4.8	7.2
2420 Willowbrae	9	0		2.5	1.8	3.1
2512 Mountcastle	48	0		2.3	1.5	2.7
2525 Crawley Ridge	11	1		2.6	1.1	2.8
2539 Dymchurch	11	2		1.3	1.4	2.0
2547 Luqa	73	18		2.5	2.7	3.6
2573 Genoa 1	12	2		10.1	11.2	15.0
2577 Cape Kinetheodolite	56	9		1.5	2.0	2.5
2586 Meudon 2	15	4		4.1	3.1	5.1
3101 Meudon	60	11		3.7	3.1	4.8
3103 Bordeaux	21	0		1.9	2.2	2.9
8030 Meudon Camera	28	7		0.10	0.07	0.12
Others	176	55				
TOTAL	1458	177				

*Geocentric.

10 observations each with a residual of 1 minute of arc together with 2 observations each with a residual of 7 minutes of arc give an rms of 3 minutes, which is a poor approximation to the observer's obvious capability of achieving 1 minute. A better measure of the observer's capability is the abc residual (average in best conditions) the arithmetic mean of the residuals on the best 70% of the observations. The abc residual is usually about half the rms residual¹⁰.

6 CONCLUSIONS

The 28 orbits of 1969-2GB determined using the PROP5 program are of very good accuracy, particularly when observations were available from the Malvern Hewitt camera or the Meudon camera. One of the orbits, No.14, with sd in eccentricity of 0.00001 and in inclination of 0.0001° , has the lowest sd yet obtained for such a high-drag orbit ($\dot{n} = 2.6 \text{ deg/day}^2$); while orbit No.7 has sd in inclination of 0.00006° .

The values of inclination, after correction for luni-solar perturbations and odd zonal and tesseral harmonics in the geopotential, have been used to determine zonal wind speeds in the upper atmosphere at heights of 210-250 km, averaged over latitudes up to about 25° . To fit theoretical curves to the observed values of inclination, the data has to be split into 3 parts, each with a different value for the atmospheric rotational speed. The results show a clear distinction between the zonal wind at night (21 h to 03 h), which is west-to-east with average speed $140 \pm 50 \text{ m/s}$, and the wind by day (04 h to 19 h), which is east-to-west with average speed $110 \pm 50 \text{ m/s}$.

10 observations each with a residual of 1 minute of arc together with 2 observations each with a residual of 7 minutes of arc give an rms of 3 minutes, which is a poor approximation to the observer's obvious capability of achieving 1 minute. A better measure of the observer's capability is the abc residual (average in best conditions) the arithmetic mean of the residuals on the best 70% of the observations. The abc residual is usually about half the rms residual¹⁰.

6 CONCLUSIONS

The 28 orbits of 1969-20B determined using the PROP5 program are of very good accuracy, particularly when observations were available from the Malvern Hewitt camera or the Meudon camera. One of the orbits, No.14, with sd in eccentricity of 0.00001 and in inclination of 0.0001° , has the lowest sd yet obtained for such a high-drag orbit ($\dot{n} = 2.6 \text{ deg/day}^2$); while orbit No.7 has sd in inclination of 0.00006° .

The values of inclination, after correction for luni-solar perturbations and odd zonal and tesseral harmonics in the geopotential, have been used to determine zonal wind speeds in the upper atmosphere at heights of 210-250 km, averaged over latitudes up to about 25° . To fit theoretical curves to the observed values of inclination, the data has to be split into 3 parts, each with a different value for the atmospheric rotational speed. The results show a clear distinction between the zonal wind at night (21 h to 03 h), which is west-to-east with average speed $140 \pm 50 \text{ m/s}$, and the wind by day (04 h to 19 h), which is east-to-west with average speed $110 \pm 50 \text{ m/s}$.

A

Table 1 - ORBITAL PARAMETERS FOR COSMOS 26

Run	MJD	Date	a	e	i	ω
1	40316.0	1969 April 5	7496.878 2	0.11919 1	48.4005 19	199.609 6
2	40328.0	1969 April 17	7468.866 2	0.11570 4	48.3998 22	152.943 6
* 3	40335.0	1969 April 24	7455.106 6	0.11411 2	48.3955 6	125.488 5
* 4	40341.0	1969 April 30	7444.314 2	0.11303 8	48.3944 7	101.828 6
* 5	40347.0	1969 May 6	7434.111 4	0.11213 10	48.4014 37	78.052 12
6	40354.0	1969 May 13	7421.192 3	0.11086 6	48.3976 25	50.198 7
** 7	40405.0	1969 July 3	7321.433 < 1	0.09902 5	48.3848 1	201.979 1
** 8	40411.0	1969 July 9	7311.948 1	0.09782 12	48.3835 4	176.972 4
9	40420.0	1969 July 18	7299.095 2	0.09601 22	48.3872 38	139.203 11
10	40434.0	1969 Aug 1	7287.498 3	0.09426 2	48.3878 23	80.214 4
11	40442.0	1969 Aug 9	7279.018 4	0.09339 3	48.3850 26	46.355 3
12	40456.0	1969 Aug 23	7260.514 2	0.09170 1	48.3824 16	346.754 3
13	40484.0	1969 Sept 20	7210.246 3	0.08618 3	48.3732 13	225.671 5
**14	40492.0	1969 Sept 28	7193.531 2	0.08385 1	48.3740 1	190.574 4
15	40497.0	1969 Oct 3	7180.211 4	0.08224 4	48.3768 14	168.469 3
16	40503.0	1969 Oct 9	7166.513 2	0.07995 4	48.3719 20	141.800 4
17	40522.0	1969 Oct 28	7126.262 2	0.07445 2	48.3738 19	56.312 4
* 18	40532.0	1969 Nov 7	7102.478 2	0.07172 3	48.3727 5	10.687 2
19	40539.0	1969 Nov 14	7083.106 3	0.06966 2	48.3684 15	338.432 2
20	40554.0	1969 Nov 29	7033.314 3	0.06410 2	48.3603 19	268.202 3
21	40561.0	1969 Dec 6	7009.216 3	0.06129 3	48.3605 16	234.832 7
22	40574.0	1969 Dec 19	6963.248 2	0.05524 1	48.3529 13	171.854 3

Table continued on page 14. For key to symbols, see page 14.

B

ERS FOR COSMOS 258 ROCKET (1969-20B) WITH STANDARD DEVIATION

	Ω	ω	M_0	M_1	M_2	M_3	M_4	ϵ	N	D
006	199.609	205.13	22.67	4814.414	1.2122	-0.0066	-	0.85	47	8.4
19	6	1	1	2	4	1				
998	152.943	247.54	1.10	4841.521	1.0736	-0.0089	-0.00100	0.91	55	8.9
22	6	2	3	2	11	2	6			
55	125.488	272.67	99.72	4854.929	0.8690	-	-	1.01	42	5.1
6	5	3	3	6	15					
944	101.828	294.10	100.72	4865.490	0.8916	-0.0124	-	0.84	32	4.0
7	6	7	8	2	29	16				
014	78.052	315.99	163.56	4875.508	0.8306	0.0062	-	1.01	30	7.0
37	12	7	9	4	19	4				
976	50.198	340.95	135.50	4888.244	1.0513	0.0280	-	0.93	32	5.3
25	7	2	2	3	30	7				
848	201.979	168.64	163.05	4988.478	0.7726	-	-	0.52	19	2.1
1	1	1	< 1	< 1	1					
835	176.972	191.22	242.74	4998.186	0.8400	-0.0048	-	0.88	54	7.1
4	4	1	1	1	6	1				
872	139.203	25.58	289.87	5011.393	0.5211	-0.0167	0.00090	0.69	66	7.0
38	11	3	4	2	12	2	9			
878	80.214	279.48	334.96	5023.359	0.4299	0.0066	-	0.78	45	4.9
23	4	2	2	3	10	6				
850	46.355	310.36	234.51	5032.139	0.6544	0.0073	-	0.67	37	3.9
26	3	2	2	4	20	17				
824	346.754	4.56	256.18	5051.385	0.7677	0.0145	-	0.70	35	4.7
16	3	1	1	2	5	4				
732	225.671	113.75	229.66	5104.295	0.9676	0.0137	-	1.00	41	7.0
13	5	3	2	3	12	1				
740	190.574	145.39	92.78	5122.095	1.2768	0.0556	-	0.79	51	4.0
1	4	1	1	2	21	8				
768	168.469	165.36	179.48	5136.352	1.2980	-0.0289	0.00267	0.92	58	5.0
14	3	1	1	5	15	23	54			
719	141.800	189.64	81.69	5151.084	1.2183	0.0100	-	0.94	47	5.2
20	4	2	2	2	18	5				
738	56.312	267.99	88.08	5194.782	1.2694	0.0043	-0.00067	0.83	71	8.2
19	4	2	3	2	11	2	6			
727	10.687	309.78	324.40	5220.893	1.3519	0.0119	0.00553	0.92	60	5.1
5	2	2	2	3	19	5	24			
84	338.432	339.32	224.26	5242.323	1.6193	-	-	0.58	41	3.3
15	2	1	1	3	14					
603	268.202	43.22	56.65	5298.083	2.0350	-0.0085	0.00178	0.95	37	5.0
19	3	1	2	3	22	7	37			
605	234.832	73.48	159.57	5325.426	2.0297	-0.0003	-0.00718	1.04	40	5.3
16	7	3	3	3	28	6	41			
529	171.854	130.01	239.72	5378.239	2.3276	0.0165	0.00280	1.18	68	7.6
13	3	1	2	2	10	2	7			

REFERENCES

- | <u>No.</u> | <u>Author(s)</u> | <u>Title, etc.</u> |
|------------|-----------------------------------------------|-----------------------------------------------------------------------------------------------------------------------------------------------------------------------------------------------------------------|
| 1 | R.H. Gooding
R.J. Tayler | A PROP3 users' manual.
RAE Technical Report 68299 (1968) |
| 2 | D.G. King-Hele
G.E. Cook
D.W. Scott | Evaluation of odd zonal harmonics in the geopotential, of degree less than 33, from analysis of 22 satellite orbits.
<i>Planet. Space Sci.</i> , <u>17</u> , 629 (1969)
RAE Technical Report 68202 (1968) |
| 3 | G.E. Cook | PROD, a computer program for predicting the development of drag-free satellite orbits. Part 1: theory.
RAE Technical Report 71007 (1971) |
| 4 | D.G. King-Hele
D.W. Scott | Further determinations of upper-atmosphere rotational speed from analysis of satellite orbits.
<i>Planet. Space Sci.</i> , <u>15</u> , 1913 (1967)
RAE Technical Report 67179 (1967) |
| 5 | D.G. King-Hele
R.R. Allan | The rotational speed of the upper atmosphere: a review.
<i>Space Science Rev.</i> , <u>6</u> , 248 (1966)
RAE Technical Report 66212 (1966) |
| 6 | D. Rees
R.W. Roper
K.H. Lloyd
C. Low | High-altitude profiles of wind velocity, temperature and density.
Paper presented at COSPAR meeting, Prague, 1969 |
| 7 | J.F. Bedinger | Measurements of winds above 200 km.
<i>Journ. Geophys. Res.</i> , <u>75</u> , 683 (1970) |
| 8 | M. Ackerman
E. Van Hemelryck | Measurement of upper atmospheric winds at 160 and 275 km.
<i>Journ. Geophys. Res.</i> , <u>76</u> , 3162 (1971) |
| 9 | D.G. King-Hele
D.W. Scott | Rotational speed of the upper atmosphere, from the orbits of satellites 1966-51A, B and C.
<i>Nature</i> , <u>213</u> , 1110 (1967) |
| 10 | H. Hilier | Determination of the orbit of Cosmos 307 rocket and its use in atmospheric research.
RAE Technical Report 71151 (1971) |

REFERENCES (Contd)

- | <u>No.</u> | <u>Author(s)</u> | <u>Title, etc.</u> |
|------------|------------------|-----------------------------------------------------------------------------------------------------------------------------------------------------------------------------|
| 11 | R.A. Challinor | Neutral-air winds in the ionospheric F-region for an asymmetrical global pressure system.
<i>Planet. Space Sci.</i> , <u>17</u> , 1097 (1969); <u>18</u> , 1485 (1970) |
| 12 | D.G. King-Hele | Measurements of upper-atmosphere rotational speed from changes in satellite orbits.
RAE Technical Report 71171 (1971) |
| 13 | D. Rees | Ionospheric winds in the auroral zone.
<i>Journ. Brit. Interplan. Soc.</i> , <u>24</u> , 233 (1971) |
| 14 | R.H. Gooding | Lumped geopotential coefficients $\bar{C}_{15,15}$ and $\bar{S}_{15,15}$ obtained from the resonant variation in the orbit of Ariel 3.
RAE Technical Report 71068 (1971) |
| 15 | D.W. Scott | ORES: a computer program for the analysis of residuals from FPOP.
RAE Technical Report 69163 (1969) |



Fig.1 Values of perigee distance a (1-e) relative to Earth of radius R (=6378.2 km) φ .

Fig. 2

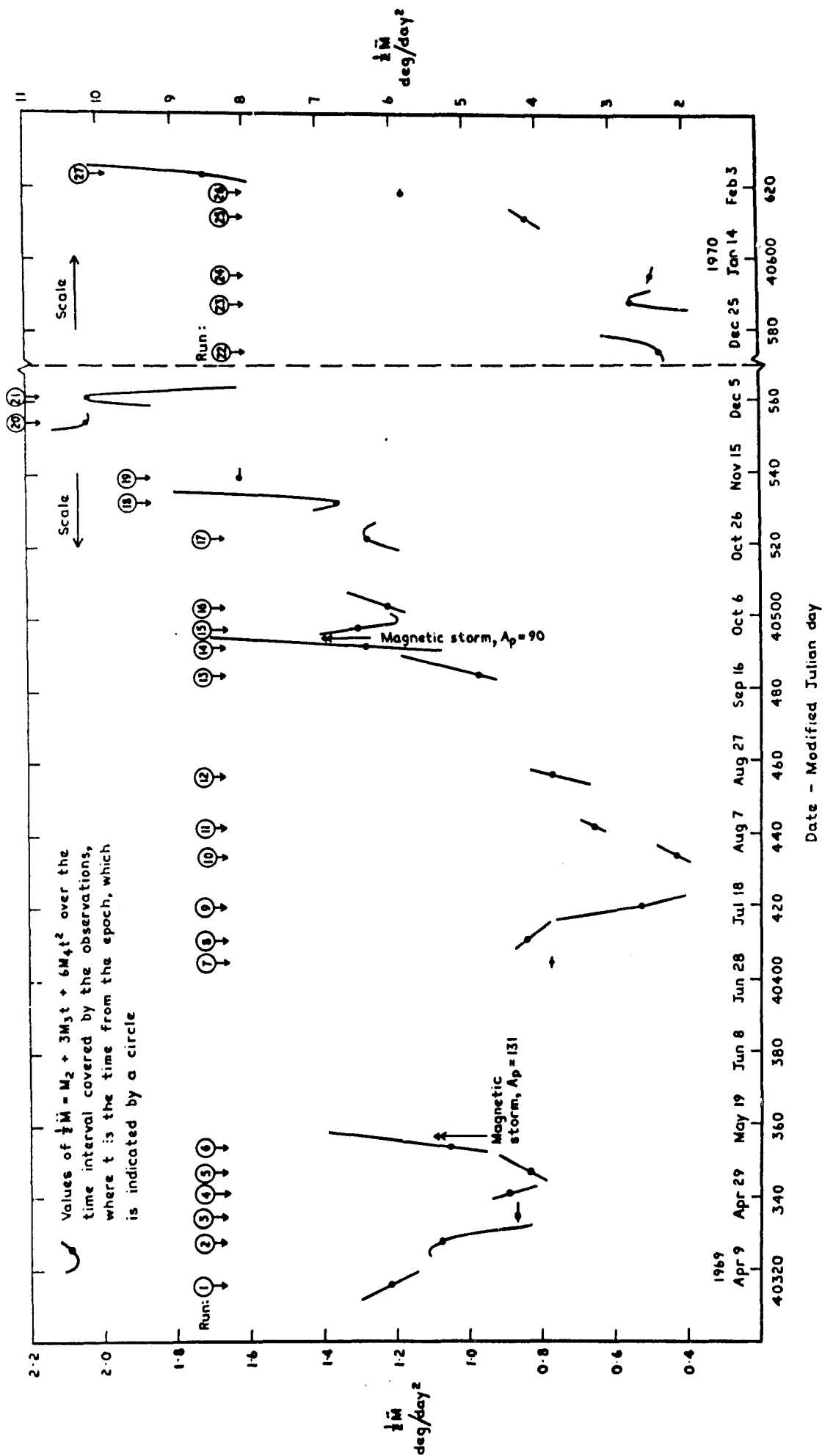


Fig. 2 Values of $\frac{1}{2}\dot{M}$ given by the orbits (excluding the last)

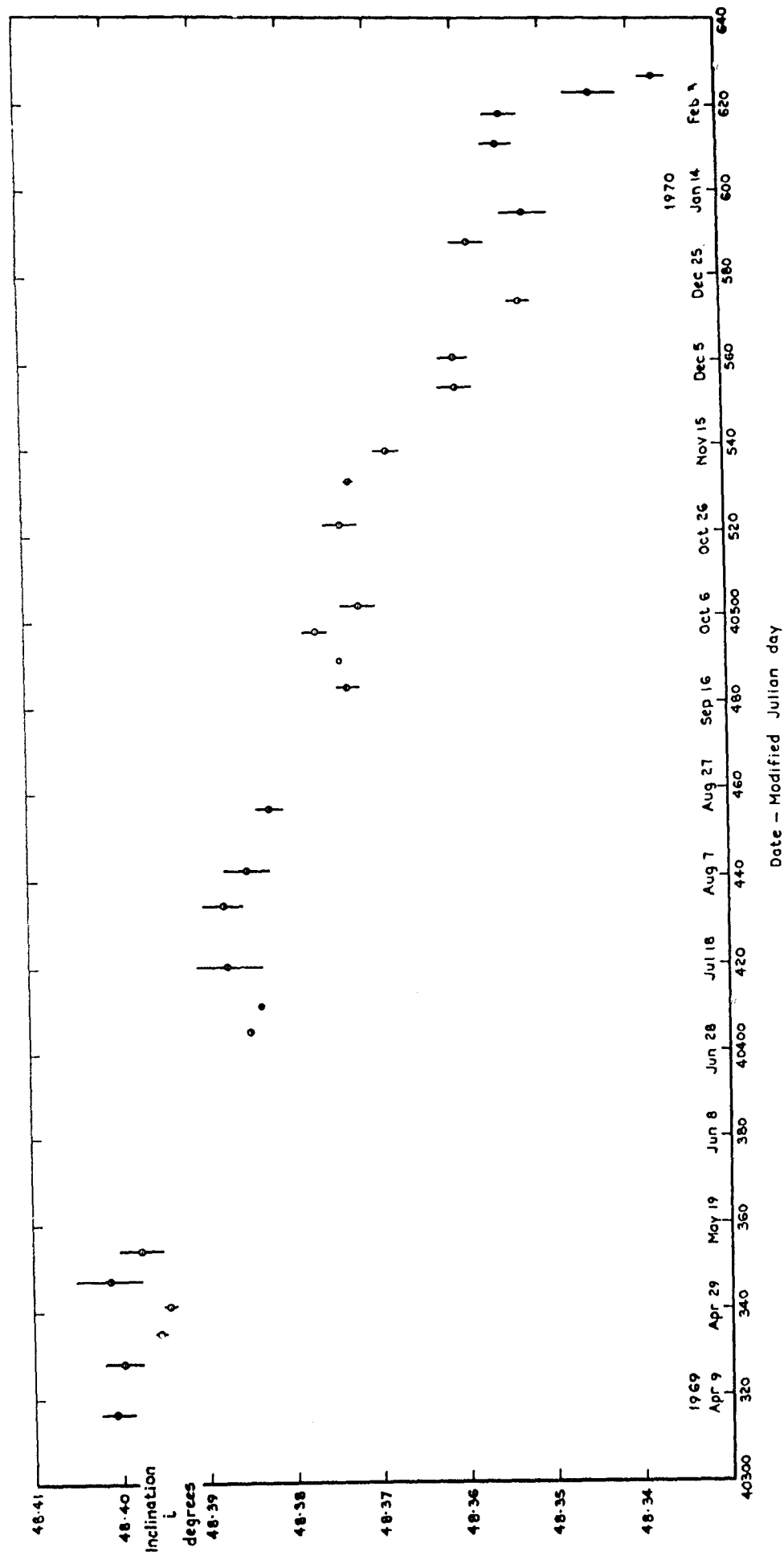


Fig.3 Values of orbital inclination i on the 28 orbits, with sd

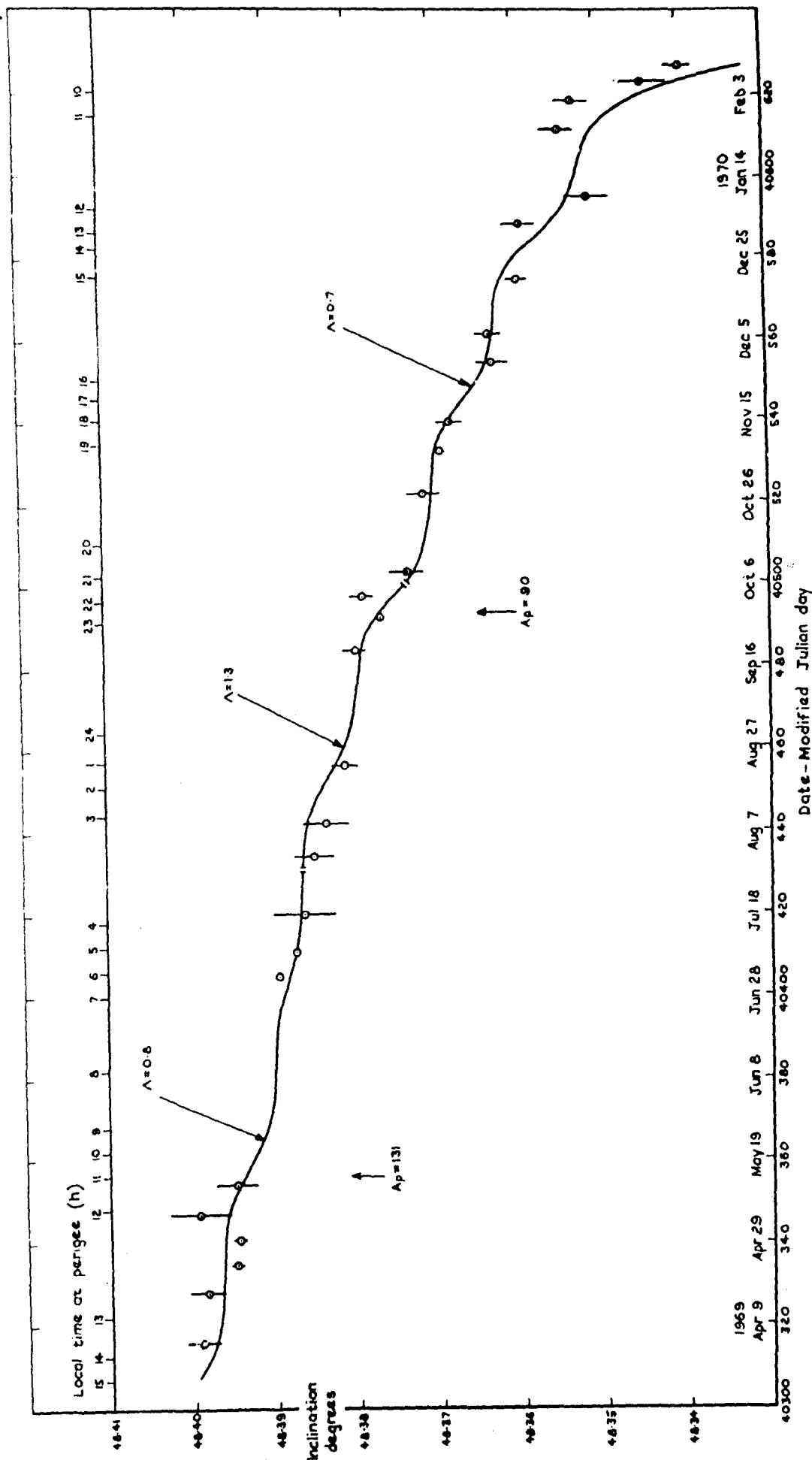


Fig.4 Values of inclination corrected for luni-solar, zonal and tesseral harmonic perturbations, with fitted theoretical curves